Complexes of Glucoamylase with Maltoside Heteroanalogues: Bound Ligand Conformations by Use of Transferred NOE Experiments and Molecular Modeling†

Thomas Weimar,‡ Bjarne Stoffer,§ Birte Svensson,|| and B. Mario Pinto*,⊥

Institut für Chemie, Medizinische Universität zu Lübeck, Ratzeburger Allee 160, Lübeck 23538, Germany, Royal Danish School of Pharmacy, Department of Medicinal Chemistry, Universitetsparken 2, Copenhagen DK-2100, Denmark, Department of Chemistry, Carlsberg Laboratory, Gamle Carlsberg Vej 10, Valby DK-2500, Denmark, and Department of Chemistry, Simon Fraser University, Burnaby, British Columbia V5A 1S6, Canada

Received July 16, 1999; Revised Manuscript Received October 27, 1999

ABSTRACT: Transferred nuclear Overhauser effect (trNOE) experiments have been performed to investigate the conformations of the competitive inhibitors, methyl 5′-thio-4-*N*-α-maltoside **3a** and methyl 5′-thio-4-*S*-α-maltoside **4** when bound to the catalytic subunit of the enzyme glucoamylase. These NMR data suggest that, although each of the free ligands populates two conformational families, both heteroanalogues are bound by the enzyme in conformations in the area of the global energy minimum. These conformations have been used as initial points for docking into the active site of the enzyme taken from a X-ray crystal structure of the related glucoamylase-D-gluco-dihydroacarbose **2** complex. Minimization of the resulting complexes has yielded structures for the bound complexes. Corroboration of the structures is provided by fast $T_{1\rho}$-relaxation effects for certain ligand protons as a result of close contacts with protons in the enzyme active site. The results auger well for the combined use of transferred NOE spectroscopy and molecular modeling based on X-ray crystal structures of complexes of suitable congeners for the rapid analysis of ligand−receptor interactions.

Glucoamylase is an exo-acting inverting glycoside hydrolase (α-1,4-D-gluco-glucanohydrolase) that catalyzes the release of *β*-D-glucose from the nonreducing ends of starch and related poly- and oligosaccharides (*1*). The three-dimensional structure of the N-terminal proteolytic form of *Aspergillus awamori* var. X100 glucoamylase containing a catalytic $(\alpha/\alpha)_6$-domain and a 30 residues O-glycosylated C-terminal extension (referred to as CD)[1] has been determined at 2.3 Å resolution (*2*, *3*). In the intact larger form of the enzyme (G1), this C-terminal segment is followed by a highly *O*-glycosylated 40 residues linker to a C-terminal starch binding domain (*4*). Another naturally occurring form (G2) lacks the starch binding domain, but contains the full length linker region (*5*). The enzyme has a funnel-shaped active site and was shown kinetically to interact with substrate glucosyl residues at seven consecutive subsites, with cleavage occurring between subsites −1 and +1 (*6*, *7*). In the crystal structures of complexes with the pseudotetrasaccharide inhibitors acarbose **1** (*8*, *9*) (Scheme 1) and D-gluco-dihydroacarbose (GAC) **2** (*9*, *10*), protein sugar contacts are

Scheme 1

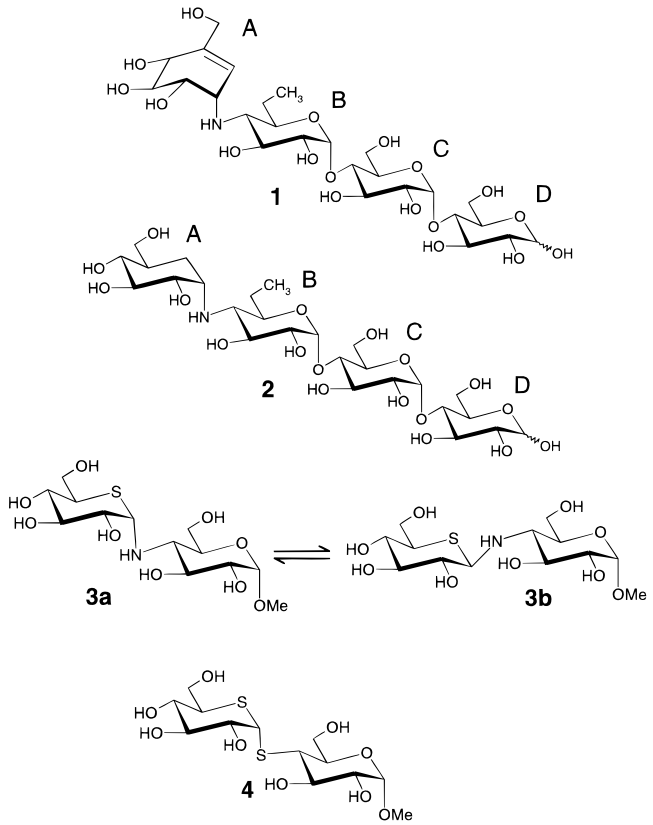

† This work was supported with grants from the Deutsche Forschungsgemeinschaft, the Fonds der Chemischen Industry (both to T.W.), NATO (CRG # 931165), and the Natural Sciences and Engineering Research Council of Canada.

* To whom correspondence should be addressed. Telephone: ++1-604-291-4327. Fax: ++1-604-291-3765. E-mail: bpinto@sfu.ca.

‡ Institut für Chemie. Telephone: ++49-451-4219. Fax: ++49-451-4241. E-mail: thomas.weimar@chemie.mu-luebeck.de.

§ Royal Danish School of Pharmacy.

|| Carlsberg Laboratory. Telephone: ++45-33-27-53-45. Fax: ++45-33-27-47-08. E-mail: bis@crc.dk.

⊥ Simon Fraser University.

[1] Abbreviations used: G1, glucoamylase 1; G2, glucoamylase 1 without the starch binding domain; GAC, D-gluco-dihydroacarbose; CD, catalytic domain; gg, gauche gauche; gt, gauche trans; τ_c, rotational correlation time; trNOE, transferred NOE; NOE, nuclear Overhauser effect; rms, root-mean-square; ROE, rotating-frame Overhauser effect.

10.1021/bi991645i CCC: $19.00
Published on Web 12/15/1999

found for the innermost four subsites in the complex. Depending on the pH, two different binding modes are observed for the reducing maltosyl unit (residues C and D), whereas the terminal residues A and B superimpose in all structures.

As part of a program to evaluate the potential of heteroanalogues of oligosaccharides as glycosidase inhibitors, we have described the synthesis, conformational analysis, and enzyme inhibitory activity of heteroanalogues of disaccharides in which the ring oxygen and/or the interglycosidic oxygen atoms are replaced by sulfur, selenium or nitrogen (*11*−*13*). Of particular interest for the design of more effective carbohydrase inhibitors and carbohydrases or the understanding of subtle events in the catalytic mechanisms of the enzymes is a knowledge of the nature of the interactions in complexes of carbohydrases with their inhibitors. Such knowledge may be obtained by X-ray crystallography but an alternative protocol in which the bound inhibitor conformations in solution are assessed by transferred NOE NMR experiments (*14*−*20*) prior to their docking into the enzyme active sites, known from X-ray crystallographic studies of related complexes, also has merit.

We have reported preliminary transferred NOE data for a complex of the α-isomer of maltoside heteroanalogue **3a**, containing sulfur in the ring and nitrogen in the interglycosidic linkage with glucoamylase (G1) from *Aspergillus niger* (*11*). We report herein a detailed analysis of the bound conformations of **3a** and a second analogue **4** in which the interglycosidic atom is sulfur. We report also the docking of the trNOE-derived conformations of **3a** and **4** into the crystal structure of the catalytic domain of glucoamylase (CD), the minimization of the resulting complexes, and analysis of the ligand conformations and protein−ligand contacts. Compounds **3a** and **4** are competitive inhibitors of the hydrolysis of maltose by glucoamylase (*11*, *12*) and are envisaged to mimic rings A and B of acarbose and GAC.

MATERIALS AND METHODS

NMR Experiments. NMR experiments were performed on an AMX 600 spectrometer (Bruker) equipped with an inverse triple-probe with the program UXNMR (Bruker). D_2O buffers (phosphate-buffered saline: 50 mM pH 7.2 for **3**. acetate buffer: 50 mM CD_3CO_2Na pH 4.5 for **4**; both buffers are not corrected for kinetic isotope effects) were used as solvents in centriprep concentrators (Amicon) to remove exchangeable protons of G1 (M_W 82 700). Phosphate buffer was used for the case of **3**, because of the concern of the stability of **3** in acetate buffer. Samples of glucoamylase G1, prepared as described by Stoffer et al. (*21*), with concentrations of 16.6 mg in 450 μL phosphate buffer (200 nmol) and 12.4 mg in 450 μL acetate buffer (145 nmol) were prepared for the trNOE experiments. These samples were titrated with stock solutions of **3** and **4**, respectively. During the titration, the magnitudes of the observed trNOEs were monitored with selective 1D transient NOE experiments, performed on the resonance of H1′ of both inhibitors. This gave final sample volumes of ∼560 μL with a ratio of **3a**:**3b**:G1 of ∼25:65:1 (in phosphate buffer) and ∼470 μL with a ratio of **4**:G1 of ∼27.5:1 (in acetate buffer). Subsequently, the experimental temperatures were optimized to give the maximum trNOEs. This resulted in temperatures of 288 and 284 K for the samples of **3** and **4** with G1, respectively. For the trNOE experiments, a modified NOESY pluse-sequence incorporating a spin-lock filter (*22*) (18 ms, 15 dB) after the first 90° pulse to relax the protein resonances, and a homospoil pulse in the middle of the mixing time were used. Presaturation of residual water was used to suppress solvent signals during the relaxation. TrNOE experiments were performed with mixing times of 30, 80, 140, 200, and 250 ms for the mixture of **3a**, **3b**, and G1 and mixing times of 30, 50, 100, 150, and 200 ms for the mixture of **4** and G1. ROESY experiments used spin-lock times of 30, 100, and 200 ms or 50, 100, and 200 ms for the samples of **3** and **4** with G1, respectively. Experimental data (2K × 512) were Fourier transformed to give final data matrixes of 4K × 1K data points; the trNOE effects were integrated and converted into experimental distances with Aurelia (Bruker) and, additionally, using the isolated spin-pair approximation. Both methods showed good agreement. 1D-transient NOE experiments and data treatment were performed as described (*23*, *24*).

Molecular Modeling. Interproton distances from the trNOE experiments were used as restraints in an energy minimization of free **4** with Sybyl (Tripos) using the standard Sybyl force-field and a penalty function constant of 200 kcal/mol Å^2. Therefore, the distances between the protons H1′−H4, H4−$H6_{pro}S$ and H5′−$H6_{pro}S$ were defined to be in a range of 2.55−2.7, 2.7−2.9, and 2.6−2.8 Å, respectively. The interglycosidic trNOE H1′−H4 in **3a** gave an experimental distance for this contact in the range of ∼2.3−2.5 Å, which corresponds to the global minimum energy conformation found with the Sybyl force-field without additional restraints. Assuming the same binding mode for **3a** as for **4**, the hydroxymethyl group was also rotated into the gt-position in **3a**. These two trNOE derived-conformations were subsequently used in a docking procedure together with the high-resolution structure of the D-gluco-dihydroglucoacarbose complex of the catalytic domain of glucoamylase (*9*) (1.7 Å resolution, including water molecules) to generate models for the disaccharide complexes. Therefore, the nonreducing ring of the trNOE-derived conformations of **3a** and **4** were superimposed upon the A-ring of GAC using the atoms C2, C3, and C4. The nonreducing ring of **4** superimposed with a rms. value of 0.041 Å whereas the equivalent ring of **3a** superimposed with a rms value of 0.035 Å. The glycosidic dihedral angles ϕ and ψ of **3a** and **4** were adjusted to account for unfavorable van der Waals contacts to G2. Furthermore, the OH6 groups at the nonreducing end of **3a** and **4** were adjusted to the orientation of the equivalent group of GAC in the complex structure.

After construction of the complexes of the catalytic domain of glucoamylase (CD) with the inhibitors **3a** and **4** hydrogen atoms were added to the complexes (including the complex of GAC with CD), assuming a pH of 7.2 for the complex of **3a** and 4.2 for the complex of **4** using INSIGHTII (Molecular Simulations). Finally, the complexes were soaked in a water layer of 2.5 Å to fill out holes and to create uniform surfaces of all three complexes. The complexes were then minimized using DISCOVER (Molecular Simulations) for 6000 iterations using the steepest descent algorithm and the force-field cff91. A double cutoff value of 20 and 25 Å was used in these energy calculations to reduce computational time. To account for the trNOE data in **4**, the distance between the

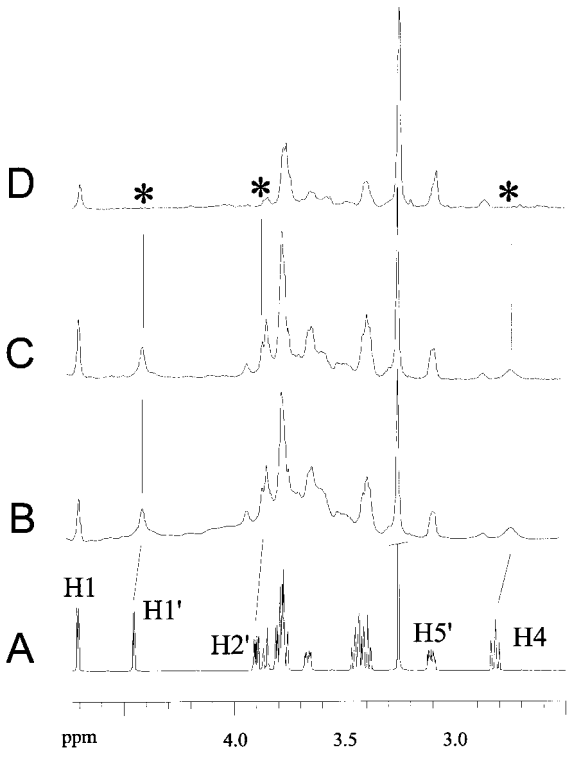

FIGURE 1: 1D NMR spectra of **4** in D_2O and in the mixture with G1: (A) 1D spectrum of **4**. (B) 1D spectrum in a mixture with G1. (C, D) $T_{1\rho}$-filtered spectra of the mixture with $T_{1\rho}$-filters of 16 ms and 200 ms, respectively. The signals H1′, H2′, and H4 show faster relaxation behavior than the rest of the disaccharide signals and are marked with an asterisk.

protons H1′ and H4 was restrained from 2.21−2.87 Å with a target distance of 2.54 Å and that between the protons H5′ and $H6_{pro}S$ from 2.20−3.38 Å with a target distance of 2.59 Å, with a constraint factor of 200 kcal/mol Å^2. The same procedure was used for the complex of **3a** with a pH of 7.2 and one distance restraint with an interval of 2.30−2.50 Å and a target distance of 2.40 Å for the interglycosidic contact between protons H1′ and H4.

RESULTS AND DISCUSSION

NMR-experiments. The overall rotational correlation time (τ_c) of medium sized or large proteins has a severe impact on the NMR spectra of such compounds. The slow tumbling causes a fast T_2- and $T_{1\rho}$-relaxation that, in turn, yield large line widths of the protein resonances that cannot be resolved in normal NMR experiments. These relaxation effects can be used to suppress the protein background signals prior to acquisition by incorporating a T_2- (*25*) or $T_{1\rho}$-filter (*22*) into the pulse sequence. Since the ligand molecules usually show T_2-relaxation times in the range of several hundred milliseconds, these filters suppress the protein signals very effectively within milliseconds without seriously affecting the resonances of the ligand. We used a $T_{1\rho}$-filter in 1D and 2D experiments to relax the protein signals within 16 ms (Figure 1). It is interesting to note that some carbohydrate resonances of the glycoprotein, especially in the anomeric region, are still observable with $T_{1\rho}$-filters of 50 or 100 ms length (spectra not shown). The $T_{1\rho}$-relaxation behavior of these resonances is, therefore, closer to the behavior of the ligand than of the protein and has to be interpreted in terms of a mobility (correlation time) in water that is higher for the carbohydrate portion of the glycoprotein than for the protein portion. Since the overall correlation time is the same for both portions of the glycoprotein, it follows that the carbohydrate must have local motions on a time scale that is faster than the overall motion of the glycoprotein.

The relationship of inhibitors **3a** and **4** to the parent molecule methyl α-D-maltoside is realized by the fact that these three compounds populate similar conformational families at the α-(1−4) glycosidic linkage (*13*, *26*, *27*). The most profound difference between these compounds is the different distribution of conformations between global and local minimum energy regions. A preliminary report of the enzyme-bound conformation of **3a** indicated that, although the compound populates both local and global minimum conformations, it is bound by glucoamylase G1 in a conformation in the area of the global minimum of the free disaccharide (*11*).

Addition of the inhibitors to a solution of G1 gave rise to line broadening effects for the inhibitor proton resonances. The general line broadening effect of the inhibitor resonances points to an intermediate kinetic exchange rate between the free and the enzyme-bound states of the inhibitors. Line-broadening effects of similar magnitudes have been observed previously for protein-carbohydrate complexes (*28*). Although, the dissociation rate constant of the complex is unknown, the X-ray structures of complexes of CD with deoxynojirimicin (*29*), acarbose (*8*, *9*), and GAC (*9*) support such intermediate exchange behavior. Thus, the catalytic site of glucoamylase resides in a deep cleft in the center of the enzymatic subunit of glucoamylase. During the normal action of the enzyme, the oligosaccharide substrate has to move inside the cleft, whereupon the terminal unit is cleaved. After hydrolysis, the substrate chain and the released glucose unit have to dissociate out of the active site in order to initiate a new catalytic cycle.

Although all inhibitor resonances were broadened to some extent, the resonances of H4 and H1′ of **3a** and **4** displayed the most profound line broadening, accompanied by a shift in their resonance frequencies (Figure 1). Such marked shifts have been observed previously for a protein−carbohydrate complex (*30*). Application of a $T_{1\rho}$-filter (*22*) to suppress the protein background signals, also showed a faster relaxation behavior for the H4 and H1′ protons, as well as the H2′ proton, when compared to the other protons of the inhibitor. The extreme line-broadening and chemical-shift changes upon binding, together with the increased $T_{1\rho}$-relaxation behavior of the protons H1′, H2′, and H4 suggests that a special effect, superimposed on the normal exchange process, is operating here (see below).

Although the exchange rate appears to be in the intermediate regime on the chemical-shift time scale, it is fast on the T_1-relaxation time scale since trNOEs are observed for the complexes of both inhibitors with G1 (see Figure 2). The trNOE spectra of both inhibitors with G1 (Figure 2) also showed differential line broadening of the cross-peaks involving H1′ and H4. The case for **4** is simpler and will be discussed first. The trNOE spectrum of **4** that was recorded at 200 ms mixing time (Figure 2A), displayed trNOE effects that could be used to derive the bound conformation of the inhibitor. Apart from the interglycosidic effect H1′−H4, the trNOE H5′−$H6_{pro}S$ restricts the conformational freedom at

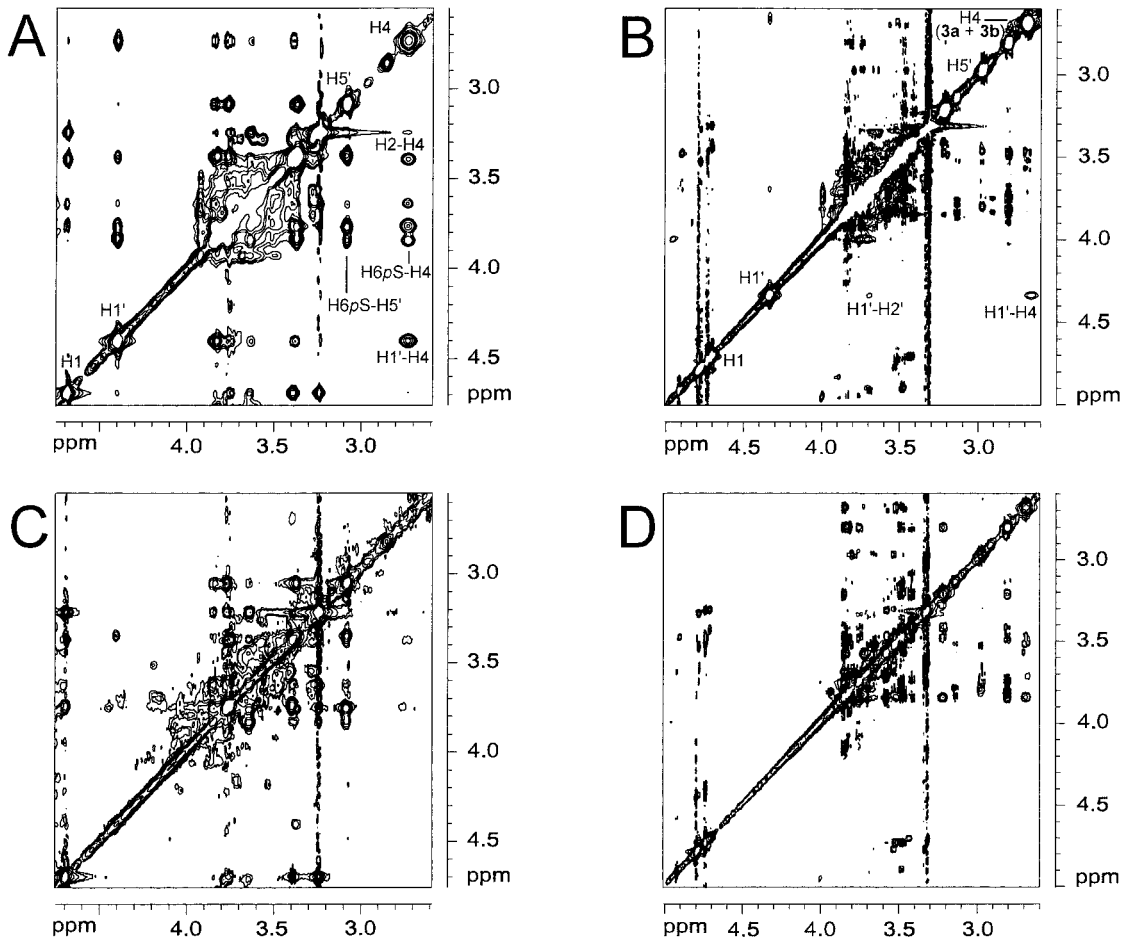

FIGURE 2: TrNOE and trROE spectra of **3a** and **4** with G1. The important effects are labeled. (A) TrNOE spectrum (200 ms mixing time) of the complex of **4** with G1. Only negative levels are plotted. (B) TrNOE- spectrum (250 ms mixing time) of the mixture of **3a** and **3b** with G1 (positive and negative levels are plotted). Only very weak trNOE effects of **3a** are visible in B. Most of the signals are zero-quantum artifacts. (C) TrROE spectrum of the complex of **4** with a spin lock time of 200 ms. Positive and negative levels are shown. The diagonal- and cross-peaks of the protons H1′ and H4 are missing. (D) trROE spectrum (200 ms spin lock) of the mixture of **3a** and **4** with G1. Positive and negative levels are plotted. The diagonal- and cross-peaks of the protons H1′ and H4 are missing. The signal of H4 of the unbound **3b** remains.

the α-(1−4) glycosidic linkage. Additional information comes from the trNOE effect H4−$H6_{pro}$S, which restricts the rotation about the C5−C6 bond in the glucose unit. Unfortunately, the line broadening effects did not permit an unequivocal assignment of the effect H4−$H6_{pro}$R in this unit. The resonance for the protons $H6_{pro}$R and -S in the 5-thio-glucose unit was degenerate so that no information about the orientation of the C5−C6 bond of this unit in the bound state could be obtained.

The trNOE spectra of **3a** (Figure 2B) were complicated by the fact, that **3a** is in slow exchange with the corresponding cellobioside heteroanalogue **3b** (*11*) in a ratio of ∼1:2.5 (**3a**:**3b**), each giving rise to a set of resonances. Since negative trNOEs were only observed for **3a**, and the cellobioside heteroanalogue **3b** displayed small positive NOEs, the trNOE spectrum permitted the discrimination between the compound bound by the enzyme, namely, **3a**, and unbound compound **3b** (*11*, *31*). The observed trNOE effects for **3a** bound by the enzyme were even smaller than those observed for bound **4**. The spectra of the complex of **3a** were further complicated by the ∼2.5 excess of **3b** and only the interglycosidic trNOE H1′−H4 could be analyzed to give a distance range of 2.3−2.5 Å for this contact. Since the overall features of the trNOE spectra of both inhibitors were similar (see Figure 2), the binding mode of **3a** was assumed to be similar to that of **4** and, therefore, both hydroxymethyl groups of **3a** were treated in the same way as for **4**.

The low signal intensity for the H1′−H4 contact most likely has its origin in the binding kinetics of complex formation. Since the observation of trNOEs depends on the dissociation rate constant (off-rate) of the complex relative to the T_1-relaxation time (*17*), the binding kinetics for the complex of **3a** seems to be in a range where trNOE effects are not substantial. We note that compound **3a** is a good competitive inhibitor of glucoamylase-catalyzed hydrolysis of maltose ($K_i = 4\ \mu M$) as compared to a $K_i = 2$ mM for **4** (*11*, *12*). The lower inhibitory potency of **4** is consistent with the trNOEs of greater magnitude than those observed for the complex of **3a**.

ROE Experiments of the Complexes. TrROE experiments were performed for both complexes to decide whether the trNOE effects are influenced by spin diffusion. As previously shown, the magnetization transfer in complexes with large proteins can be very effective and spin diffusion effects can influence trNOE effects and lead to erroneous structures (*25*,

Table 1: Selected Data for the trNOE-derived Bound Conformations of **3a** and **4** Compared to the Conformations after Energy Minimization of the Complexes

	3a		**4**		**GAC**
	trNOE-derived	minimized	trNOE-derived	minimized	minimized
H1′−H4	2.41 Å	2.30 Å	2.55 Å	2.21 Å	2.33 Å
H5′−$H6_{pro}$S	n.d.[a]	3.13 Å	2.59 Å	3.38 Å	2.68 Å[b]
H4−$H6_{pro}$S	n.d.	3.00 Å	2.91 Å	3.00 Å	3.33 Å[b]
Φ	−27°	−17°	−42°	−9°	−9°
Ψ	−26°	−1°	−18°	−13°	−11°
$\omega 1$[c]	n.r.[d]	gt	gt	gt	*b*
$\omega 2$[e]	n.r.	gg	n.r.	gg	gg

[a] n.d. − no experimental data available. [b] GAC contains a methyl group in the B ring. Distances relate to the proton in the corresponding position. [c] Orientation of the hydroxymethyl group of the reducing unit. [d] n.r. − not restrained due to a lack of experimental information. [e] Orientation of the hydroxymethyl group of the terminal unit.

32). The value of trNOE experiments in the rotating frame (trROE) is such that every magnetization transfer changes the sign of the observed effects, thereby making spin diffusion effects distinguishable from real trNOE effects. Unfortunately, the spectra obtained, especially with longer spin-lock times, showed a severe decrease in intensity of all peaks involving the protons H4 and H1′ of both inhibitors. At a spin-lock time of 200 ms, the diagonal peaks of H4 and H1′ as well as all cross-peaks involving these protons completely disappeared (compare Figures 2C and 2D). This behavior is identical to that already described in the $T_{1\rho}$-relaxation experiments (Figure 1) and prevents the use of trROE experiments as experimental checks of spin-diffusion in our case.

Models of the Inhibitor Complexes with the Catalytic Subunit of Glucoamylase (CD). Integration of the trNOEs for the complexes of the disaccharide inhibitors yielded experimental interproton distances that are listed in Table 1. Using these experimentally derived data as target distances in restrained energy minimization calculations, models of the complexed form of both inhibitors were derived. Since we desired a starting conformation that resembled that derived experimentally, the distance restraints were chosen to be quite narrow, although the stronger trNOE H1′-H4 was given a narrower range (±0.75 Å) than the weaker effects (±1.0 Å). We recognized that wider restraints might have given rise to other conformational microstates, but chose to rely on our experimental data. In each case, the bound conformations were located in the region of the global minimum energy conformation of the free maltoside analogues **3a** and **4** (*11*, *13*). The trNOE-derived conformations were subsequently docked into the active site of CD obtained from the high-resolution X-ray structure of the CD−GAC complex (*9*) by assuming that the 5-thioglucose units of both inhibitors have the same binding mode as ring A of GAC. Since no experimental data were available for the orientation of the hydroxymethyl groups in the 5-thioglucose units, the conformations of these units present in the GAC complex were used for the initial models. The docking procedure produced some unfavorable van der Waals contacts with the protein, which were corrected by adjusting the glycosidic torsion angles of **3a** and **4** to the conformation of bound GAC (see Table 1). Subsequently, missing hydrogen atoms were added to the protein, the complexes were hydrated with approximately 1050 water molecules, and the pH was adjusted to 7.2 and 4.2 for the complexes of **3a** and **4**, respectively to coincide with the conditions of the NMR experiments. The models of the complexes were than minimized in 6000 cycles with additional distance restraints to account for the trNOE-derived conformations. To differentiate conformational or structural changes in the complexes, which are due to the minimization procedure, from changes that stem from the substitution of GAC by the disaccharide inhibitors, the GAC complex was treated and minimized as was described for the disaccharide inhibitors **3a** and **4** at a pH of 4.2. After minimization, the atoms of **3a** and **4** and of ring A and B from the GAC complex superimposed almost perfectly (data not shown).

Table 1 compares selected data for **3a** and **4** from the trNOE-derived conformations with the conformations after the minimization of the complexes. Overall, the trNOE-derived data agree well with the data from the minimized structures. The difference in the pH values does not seem to influence the overall conformational features of the bound inhibitors. The deviations in the interglycosidic distances H1′−H4 (∼ 0.3 Å) between trNOE-derived and minimized structures is readily explained by the uncertainty of the experimental data. The difference (0.8 Å) between trNOE-derived and minimized model for the interglycosidic distance H5′−$H6_{pro}$S of inhibitor **4** is much larger. This distance seems to be underestimated in the trNOE-derived conformation and also influences the distance between the protons H1′ and H4. The differences in the interglycosidic distances were also reflected in the dihedral angles ϕ and ψ. Although, the deviations in the ψ-angle were small, the ϕ-angle showed changes up to 30°. At first glance, the differences in the dihedral angles for **4** seem to be quite drastic but the resulting conformation at the glycosidic linkage is still in the global minimum energy region on the potential energy map (*13*).

It must be noted here that the trNOEs for both inhibitors are very weak and that, in this respect, the neglect of additional inaccuracies in the NMR data, especially spin diffusion, is most likely the reason for the discrepancies observed between the trNOE and minimized models.

The trNOE between the protons H4 and $H6_{pro}$S in **4** dictates a gt orientation for the hydroxymethyl group at the reducing end. In the complex, this hydroxymethyl group (as well as the methyl group of GAC at the equivalent position) is surrounded by hydrophobic amino acids. The gt-orientation for the two disaccharide inhibitors **3a** and **4** does not result in adverse interactions with these hydrophobic amino acids but it also does not appear to yield additional protein-inhibitor hydrogen-bonding contacts.

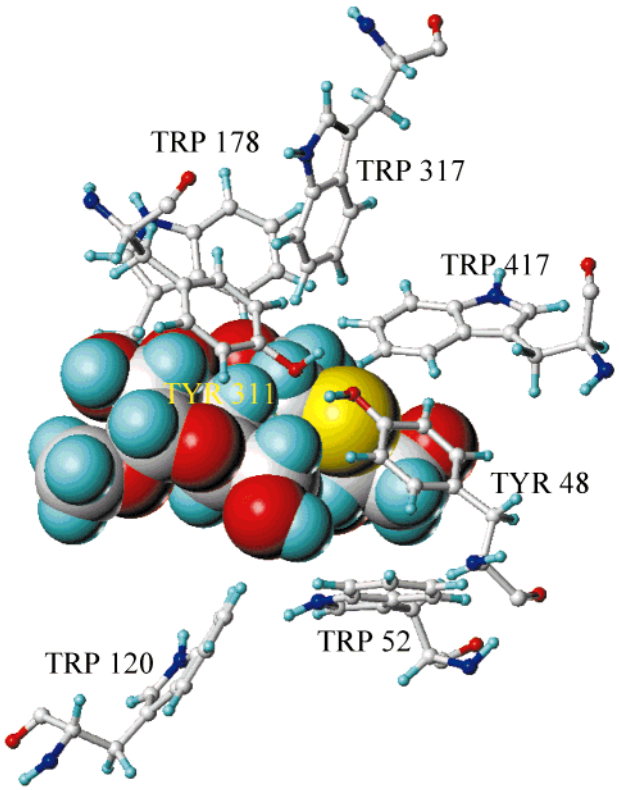

FIGURE 3: Representation of the inhibitor **4** surrounded by aromatic amino acids from the glucoamylase crystal structure. These aromatic amino acids provide favorable van der Waals and stacking interactions with the inhibitor.

Table 2: Dihedral Angles of the 5-Thioglucose Units of **3a** and **4** in Complex with Glucoamylase Compared to Those in the Solid-state Structure of **4**

	compound		
dihedral angle (deg)	**3a**	**4**	**4** (solid-state structure)[a]
C1−C2−C3−C4	−53.7	−45.8	−58.6
C2−C3−C4−C5	44.9	32.2	59.4
C3−C4−C5−C6	−162.1	−160.4	177.9
C3−C4−C5−S5	−38.6	−36.8	−62.9
C4−C5−S5−C1	37.5	48.1	59.5
C5−S5−C1−C2	−46.4	−61.4	−57.8
S5−C1−C2−C3	55.5	62.7	60.7

[a] Reference *13*.

*Analysis and Validation of the Models of the Complexes of **3a** and **4***. The general features of the complexes of both inhibitor **3a** and **4** with CD are very similiar to complexes of CD with other inhibitors described in the literature (*3*, *9*, *10*, *29*). In both complexes, the inhibitors were involved in a known hydrogen-bond network that also involved water molecules; in addition, aromatic amino acids from the protein provide a source of favorable van der Waals and stacking interactions (see Figure 3). Table 2 compares dihedral angles of the 5-thio-glucose unit of the bound inhibitors **3a** and **4** with the solid-state structure of **4**. At first glance, there seems to be a large distortion in this ring. However, such ring distortions have been observed for other complexes of CD and are known to play a crucial role in the hydrolysis of the substrate (*9*). It is important to note again that the 5-thio-glucose rings of **3a** and **4** superimposed almost perfectly with the ring A of GAC from the X-ray structure; thus, the two inhibitors fit very well into the catalytic site of the enzyme.

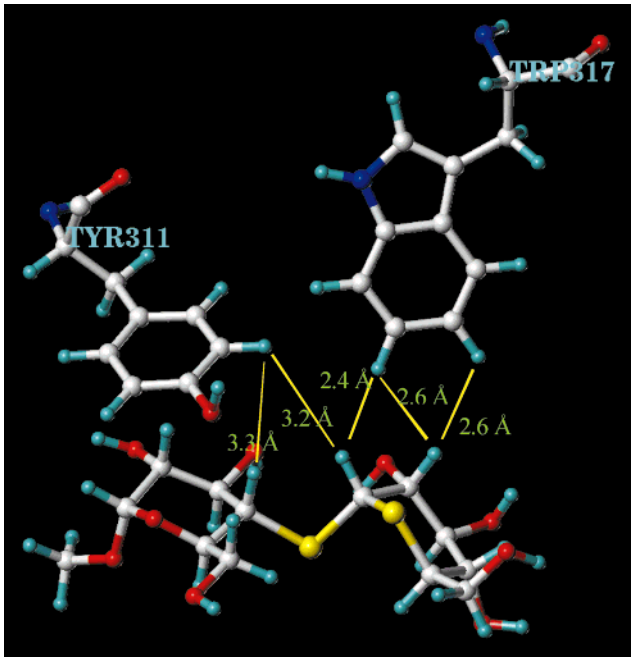

FIGURE 4: Close contacts between H1′, H2′, and H4 and aromatic amino acids Tyr311 and Trp317 of the protein in the complex of **4** with the catalytic domain of glucoamylase.

The variation in bond lengths and bond angles (relative to the oxygen congeners) that is introduced into the inhibitors through the sulfur and nitrogen atoms in the ring and the glycosidic linkage can be compensated by the variation in the dihedral angles.

The general quality of the minimized structures has to be discussed in the context of the ability of these models to explain experimental observables in solution. A reliable model would have to be in accord with specific effects and should help to interpret structural details. The models for the complexes of **3a** and **4** should, for instance, be able to account for the observed differential line broadening and relaxation behavior of the inhibitor protons H4, H1′, and H2′. Inspection of the structures of the complexes indicates that these protons in both structures are in close proximity to two aromatic amino acids (Tyr311 and Trp317), with interproton distances between some aromatic protons and the inhibitor protons being as close as 2.4 Å (compare Figures 3 and 4). In fact, these contacts are the only short distances between nonexchangeable inhibitor and protein protons found in the two complexes. From an NMR-spectroscopic point of view, these contacts, together with the long correlation time of the complex, provide a very effective source for a fast T_2- and $T_{1\rho}$-relaxation and are thus responsible for the relaxation effects discussed above.

The structures also afford an explanation for the greater inhibitory potency of **3a** versus **4**. In the structure of **3a** complexed by CD, the carboxyl function of Glu179 is within hydrogen bonding distance of the proton attached to the nitrogen atom in the glycosidic linkage. At the pH of the enzyme inhibition assays (pH 4.5) (*11*), one would expect this nitrogen atom to be protonated, and a charged hydrogen bond with the carboxylate should result. It has been suggested (*33*, *34*) that charged hydrogen bonds of this type can yield binding energies of up to ∼4 kcal/mol, which corresponds to a change in the binding constant of a factor of 1000. A charged hydrogen bond might not be the only explanation

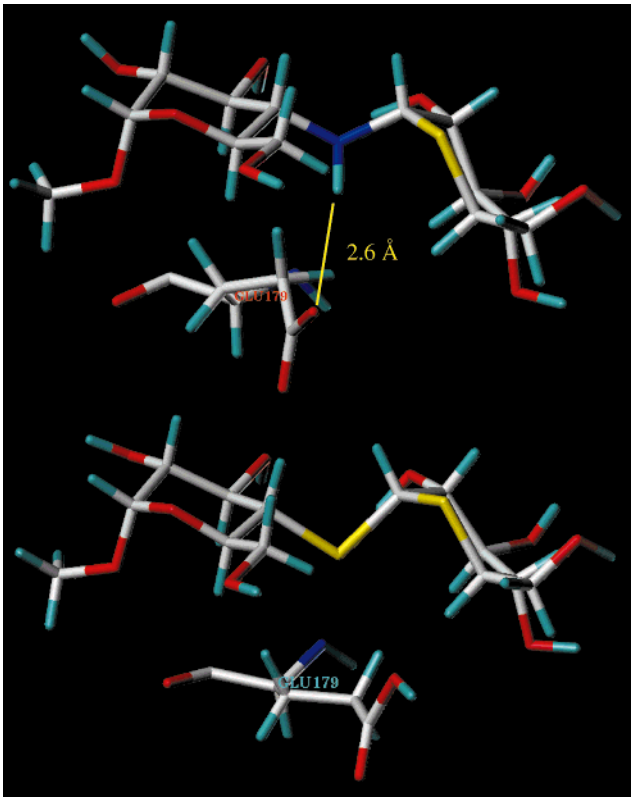

FIGURE 5: Orientation of Glu179 in the models of the complexes of the catalytic domain of glucoamylase with **3a** (top) and **4** (bottom). See text for details.

for the differences in the inhibition constants in our case, but it should certainly provide a substantial favorable energetic term for the complexation of **3a** by the enzyme G2. In contrast, in the complex of **4** with CD (pH 4.2), the entire side-chain of Glu179 is rotated away from the inhibitor and does not make any contacts with the inhibitor (Figure 5).

CONCLUSIONS

The combination of trNOE experiments and molecular modeling has been shown to be very effective in the investigation of the complexes of glucoamylase with two maltoside heteroanalogue inhibitors (**3a** and **4**). The models obtained for the complexes with the enyzme can explain specific line-broadening and $T_{1\rho}$-relaxation effects of certain inhibitor proton resonances, where short distances to protons of the enzyme yield an effective magnetization transfer. The binding features of the complexes investigated, including the selection of conformations in the global minimum energy region of the inhibitors, are in accord with the X-ray structure of the catalytic domain of glucoamylase with related inhibitors such as acarbose and D-gluco-dihydroacarbose. The principal interactions in the active site between the enzyme and the terminal ring of each of the inhibitors **3a** and **4** are with aromatic amino acids, which form extensive hydrophobic contacts. The presence of a charged hydrogen bond between the carboxylate function of Glu179 and the hydrogen atom of the interglycosidic nitrogen in **3a** can account for the greater inhibitory potency of **3a** vs the analogue **4** in which the interglycosidic atom is sulfur.

REFERENCES

1. Weill, C. E., Bursch, R J., and Van Dyk, J. W. (1954) *Cereal Chem. 31*, 150−158.
2. Aleshin, A. E., Golubev, A., Firsov, L. M., and Honzatko, R. B. (1992) *J. Biol. Chem. 267*, 19291−19298.
3. Aleshin, A. E., Hoffman, C., Firsov, L. M., and Honzatko, R. B. (1994) *J. Mol. Biol. 238*, 575−591.
4. Svensson, B., Larsen, K., Svendsen I., and Boel, E. (1983) *Carlsberg Res. Commun. 48*, 529−543.
5. Svensson, B., Larsken, K., and Gunnarson, A. (1986) *Eur. J. Biochem. 154*, 497−502.
6. Hiromi, K. (1970) *Biochem. Biophys. Res. Commun. 40*, 1−6.
7. Hiromi, K., Ohnishi, M., and Tanaka, A. (1983) *Mol. Cell. Biochem. 51*, 79−95.
8. Aleshin, A E., Firsov, L. M., and Honzatko, R. B. (1994) *J. Biol. Chem. 269*, 15631−15639.
9. Aleshin, A. E., Stoffer, B., Firsov, L. M., Svensson, B., and Honzatko, R. B. (1996) *Biochemistry 35*, 8319−8328.
10. Stoffer, B., Aleshin, A. E., Firsov, L. M:, Svensson, B, and Honzatko, R. B. (1995) *FEBS Lett. 358*, 57−61.
11. Andrews, J. S., Weimar, T., Frandsen, T. P., Svensson, B., and Pinto, B. M. (1995) *J. Am. Chem. Soc. 117*, 10799−10804.
12. Mehta, S., Andrews, J. S., Johnston, B. D., Svensson, B., and Pinto, B. M. (1995), *J. Am. Chem. Soc. 117*, 9783−9790.
13. Weimar, T., Andrews, J. S., Kreis, U. C., and Pinto, B. M. (1999) *Carbohydr. Res. 315*, 222−233.
14. Balaram, P., Bothner-By, A. A., and Dadok, J. (1972) *J. Am. Chem. Soc. 94*, 4015−4017.
15. Balaram, P., Bothner-By, A. A., and Breslow, E. (1972) *J. Am. Chem. Soc. 94*, 4017−4018.
16. Albrand, J. P., Birdsall, B., Feeney, J., Roberts, G. C. K., and Burgen, A. S. V. (1979) *Int. J. Biol. Macromol. 1*, 37−41.
17. Clore, G. M., and Gronenborn, A. M. (1982) *J. Magn. Reson. 48*, 402−417.
18. Clore, G. M., and Gronenborn, A. M. (1982) *J. Magn. Reson. 53*, 423−442.
19. Peters, T., and Pinto, B. M. (1996) *Curr. Opin. Struct. Biol. 6*, 710−719.
20. Poveda, A., Asensio, J. L., Espinosa, J. F., Martin-Pastor, M., Cañada, J. F., and Jiménez-Barbero, J. (1997) *J. Mol. Graphics Mod. 15*, 9−17.
21. Stoffer, B., Frandsen, T. P., Busk, P. K., Schneider, P., Svendsen, I., and Svensson, B. (1993) *Biochem. J. 292*, 197−202.
22. Scherf, T., and Anglister, J. (1993) *Biophys. J. 64*, 754−761.
23. Weimar, T., Meyer, B., and Peters, T. (1993) *J. Biomol. NMR 3*, 399−414.
24. Peters, T., and Weimar, T. (1994) *J. Biomol. NMR 4*, 97−116.
25. Arepalli, S. R., Glaudemans, C. P. J., Daves, G. D. Jr., Kovac, P., and Bax, A. (1995) *J. Magn. Reson. B 106*, 195−198.
26. Shashkov, A. S., Lipkind, G. M., and Kochetkov, N. K. (1986)-*Carbohydr. Res. 147*, 175−182.
27. Bock, K., Duus, J. O., and Refn, S. (1994) *Carbohydr. Res. 253*, 51−67.
28. Weimar, T., and Peters, T. (1994) *Angew. Chem., Int. Ed. Engl. 33*, 88−91.
29. Harris, E. M. S., Aleshin, A. E., Firsov, L. M., and Honzatko, R. B. (1993) *Biochemistry 32*, 1618−1626.
30. Asensio, J. L., Canada, F. J., Bruix, M., Gonzalez, C., Khiar, N., Rodriguez-Romero, A., and Jimenez-Barbero, J. (1998) *Glycobiology 8*, 569−577.
31. Meyer, B., Weimar, T., and Peters, T. (1997) *Eur. J. Biochem. 246*, 705−709.
32. Weimar, T., Harris, S. L., Pitner, J. B., Bock, K., and Pinto, B. M. (1995) *Biochemistry 34*, 13672−13681.
33. Fersht, A. T., Shi, J.-P., Knill-Jones, J., Lowe, D. M., Wilkinson, A. J., Blow, D. M., Brick, P, Carter, P., Waye, M. M. Y., and Winter, G. (1982) *Nature 314*, 235−238.
34. Davis, A. M., and Teague, S. J. (1999) *Angew. Chem., Int. Ed. Engl. 38*, 736−749.

BI991645I